Taylor & Francis
Taylor & Francis Group

The Journal of Adhesion

Improving the reversible adhesion performance of an epoxy vitrimer adhesive through surface treatment technology

Submission ID	253472701
Article Type	Original Article
Keywords	Reversible adhesives, Surface treatment, Covalent Adaptable Networks (CANs)
Authors	Marc Surós Roman, Pere Manel Verdugo Fernández, David Santiago Abraira, SILVIA DE LA FLOR

For any queries please contact:

GADH-peerreview@journals.tandf.co.uk

Note for Reviewers:

To submit your review please visit https://mc.manuscriptcentral.com/GADH

Improving the reversible adhesion performance of an epoxy vitrimer adhesive through surface treatment technology

Marc Surós[1,2], Pere Verdugo[1,3], David Santiago[1,2*], Silvia De la Flor[2*]

[1] Eurecat, Technology Center of Catalonia - Chemical Technologies Unit, c/Marcel·lí Domingo 2, 43007 Tarragona, Spain.

[2] Universitat Rovira i Virgili. Department of Mechanical Engineering, Av. Països Catalans 26, 43007 Tarragona, Spain.

[3]Universitat Rovira I Virgili. Department of Analytical and Organic Chemistry, c/Marcel·lí Domingo 1, 43007, Tarragona, Spain.

Abstract

This work evaluates the effect of different surface treatments on the adhesion and re-adhesion performance of a transesterification-based epoxy vitrimer adhesive using aluminum adherents. Although surface treatments are widely used in the adhesive industry, their role in the reversibility of vitrimer adhesion remains mostly unexplored. To quantify this effect, four adhesion methodologies were employed: pristine adhesion, re-adhesion after failure, re-adhesion after thermal debonding, and adhesion after self-welding. Various surface treatments were tested, including degreasing methods, chemical etching, and atmospheric plasma exposure. These treatments significantly enhanced the adhesion properties of the vitrimer studied, increasing pristine adhesion strength by up to 90% and re-adhesion strength by up to 130%, with certain treatments achieving full (100%) retention of the original adhesion strength. Additionally, a qualitative surface characterization is provided to explain the observed adhesion behavior.

Keywords: Vitrimers, Reversible adhesives, Surface treatment, Surface modification, Covalent Adaptable Networks (CANs), Adhesion mechanisms

1. Introduction

Adhesively bonded joints are ubiquitous: from buildings to sport equipment, even airplanes and spacecrafts. In a lot of contexts, adhesives fulfill a structural function. This is due to the great advantages offered by this bonding technique, such as the negligible weight added to the structure, a good stress distribution, the possibility of joining dissimilar materials or a highly aesthetic finish while a strong bond is formed. Additionally, adhesive joints avoid the appearance of points with high concentration of stresses [1,2]. This notwithstanding, a crucial drawback of this technology arises precisely from its primary function: the difficulty of dismantling the joints, breaking the adhesive bond, and obtaining the adherents in pristine condition. This leads to a great loss of adherent material that cannot be reused, which usually are high value-added resources. This becomes particularly concerning in sectors with high production volumes, such as the automobile industry [3]. Every year, millions of vehicles reach the end of their lifespan, posing a significant challenge for material recovery due to disassembly limitations. Traditional adhesives often complicate this process, potentially leading to the landfilling of tons of valuable metals. Similarly, the construction industry is responsible for nearly a third of global waste, much of it generated from demolition activities. Conventional thermosetting adhesives contribute significantly by creating permanent bonds that hinder material separation and recycling of building components [4].

In response to growing concerns about resource management and a circular economy, research has focused on developing debondable adhesives [5–7]. However, it proves difficult to find a way to disassemble joints without compromising on adhesion strength or making

the process too complex. A class of polymeric materials that muster most necessary properties required for reversible adhesives are vitrimers [8,9]. These polymers are able to act as thermosetting materials at operating temperatures, creating a strong and mechanically resistant bond, and at more elevated temperatures (reprocessing conditions) they acquire a malleability similar to that of thermoplastics, which allows for easy dismantling of the joints without damaging the substrates, and even re-adhesion [10]. Furthermore, this quality is granted by dynamic covalent bonds in the structure of the polymer which introduce additional reactivity to the system, which can be taken advantage of by depolymerizing through solvolysis any adhesive remains in an adequate solvent [11].

Because of these properties, many vitrimers have been proposed as reversible adhesives in the last decade [10,12–28]. Torkelson's group even proved the claim that vitrimer adhesives present higher adhesion strength than non-vitrimeric analogs [29]. These works represent great additions for reversible adhesion, however, in the authors' opinion there might be a crucial research gap in the field, as none of them adequately addresses surface preparation. In most cases it fails to be mentioned, or a relatively simplistic method is employed. Only recently, Wu et al. [30] used aluminum anodization to enhance the interface bonding strength between the aluminum alloy and the vitrimer adhesive, achieving a 130% increment in adhesion strength and enhanced reversible adhesion performance.

While there is still a debate across literature about the fundamental nature of adhesion and the inherent interactions that give rise to the adhesive bond [31], surface morphology and surface cleanliness are two key factors known to greatly influence the longevity and strength of such a bond [32]. Because of this, thorough surface preparation is an ineludible step of adhesive bonding to generate reliable joints, and it is a standard industrial practice. Proper surface preparation usually entails most of the following steps: degreasing, abrasion and (electro)chemical or plasma treatment[33,34]. Surface preparation is substrate dependent and adds complexity to the joint manufacturing process, nonetheless, it is a necessary evil as great adhesion results make up for the tedious process. Taking all this into account, one could wonder whether superficial treatment influences not only adhesion but reversible adhesion as well.

In our previous work we presented different formulations of an epoxy transesterification-based vitrimer system that could successfully be applied as reversible adhesives [35]. They presented high T_gs of around 75˚C and considerable lap-shear strengths of over 20 MPa. In addition, due to the reversible bonds in their structure they showed relatively short stress-relaxation times of about 30 minutes at 180˚C. This property allowed for their reprocessing at this temperature, which was taken advantage of with the reversible adhesion methodologies implemented. In order to further study their reversible adhesion, bond-line thickness, as a crucial adhesion parameter, was evaluated. An intriguing relationship was revealed: the thicker the bond line, the lower the lap shear strength for pristine adhesion, however, the highest re-adhesion values were obtained. Additionally, an adhesive failure was observed for the thicker bond lines, which implies a weak adhesive-surface interaction.

The combination of this tendency for higher re-adhesion values as well as the adhesive behavior of the failures, inspired us to conceive the current work, to investigate if it was possible to modify the adhesive-surface interaction and improve re-adhesion performance even further at greater bond line thicknesses.

Thus, herein, we delve into the influence of nine different superficial treatments on the re-adhesion performance of our vitrimer reversible adhesive. To do so, we used the formulation that presented the highest overall re-adhesion performance and aluminum adherents. The

superficial treatments were grouped in three different categories: degreasing, plasma and chemical etching treatments. Degreasing was evaluated as a fundamental preparation step. Ensuring a clean surface is essential for strong adhesive bonding, as the adhesive can directly adhere to the substrate without interference from contaminants. Degreasing can be used independently or as a preliminary treatment. The degreasing solution contained mild saponifiers like carbonates, phosphates, and silicates, along with a surfactant, sodium dodecyl benzene sulfonate (SDBS). The treatment was tested both with and without mechanical abrasion. Plasma treatment was employed as it is a new and promising surface treating method, which not only simplifies preparation processes but is also a cleaner alternative as it does not produce waste products and no chemicals are used [36–38]. Different exposure times were tested as well as the effect of mechanical abrasion. Finally, the chemical etching methods were included as they are usual treatment methods. Three different ones were used, firstly a nitrate etch, which is recommended in the UNE-EN ISO 13887:2004 standard, secondly a simple alkaline ultrasounds-based method developed by Saleema et al [39] and, finally, the P2 etch method which is widely used in industry as an effective chromate-free preparation method [32].

The adherents subjected to each treatment were tested in the four different adhesion methodologies: pristine adhesion, re-adhesion after break, re-adhesion after debonding and adhesion after self-welding. The lap shear strength of each was quantified, and the surfaces were qualitatively analyzed through scanning electron microscopy and water contact angle to better understand re-adhesion phenomena.

In this way, this study further demonstrates the benefits of superficial treatments on vitrimer adhesives' performance, a critical step for optimizing their application in sustainable bonding solutions. The findings could influence future strategies for improving the reversibility of adhesive joints in high-value industries.

2. Materials and methods

2.1 Materials

Diglycidyl ether of bisphenol A (DGEBA), succinic anhydride, trimethylolpropane, sodium silicate solution, sodium dihydrogen phosphate, sodium dodecylbenzenesulfonate, potassium nitrate and ferric sulfate were purchased from Sigma Aldrich (St. Louis, MO, USA). 1-methylimidazole was purchased from BASF (Ludwigshafen am Rhein, Germany). Sodium carbonate and hydrogen peroxide solution were purchased from Thermo Fischer Scientific (Waltham, MA, USA). Sodium hydroxide was purchased from Panreac Química (Castellar del Vallès, Barcelona, Spain). Sulfuric acid was purchased from Scharlab International (Sentmenat, Barcelona, Spain). Finally, acetone was purchased from Chem-Lab NV (Zedelgem, Belgium).

2.2 Vitrimer adhesive preparation

The synthesis of the vitrimer adhesive went as follows: In a vial provided with magnetic stirring, 1.0818g of succinic anhydride, 0.4835g of trimethylolpropane and 0.0555g of 1-methylimidazole were weighed and combined. The vial with this mixture was brought to 120˚C for up to 5 minutes until everything melted, and then it was left at 100˚C for 30 minutes for the reaction to take place. Next, with the vial still hot, 2.3000 g of DGEBA were added and the mixture was stirred until homogenous and transparent. At this time, it was quickly applied onto the appropriate aluminum substrates in the appropriate configuration, and it was cured in an oven for 2 hours at 120˚C, 2 hours at 160˚C and 1 hour at 180˚C. Further details can be found in reference [35].

2.3 Preparation of aluminum substrates

In order to study the effect of superficial treatments on re-adhesion, all the treatments mentioned in Table 1 were tested on Aluminum sheets (Al 6060 T66) of dimensions 100 x 25 x 2 mm. All procedures were implemented following the guidelines specified in the UNE-EN ISO 13887:2004 standard for surface preparation [40].

Table 1. Code, type and general method of each treatment evaluated in this work.

Treatment code	General method	Treatment type
T0-ref	Acetone wiping and abrasion	Previous work
T1-deg	Degreasing solution	Degreasing
T2-deg-abr	Abrasion and degreasing solution	Degreasing
T3-pla-5	Plasma exposure (5min)	Plasma
T4-pla-5-abr	Abrasion and plasma exposure (5min)	Plasma
T5-pla-10-abr	Abrasion and plasma exposure (10min)	Plasma
T6-chem-NO3	Nitrate etch (with degreasing components)	Chemical
T7-chem-alkUS	Alkaline ultrasounds etch	Chemical
T8-chem-P2	Degreasing and P2 etch	Chemical

The first step of all treatments was the cleaning of ink markings and visible organic contamination by wiping with an acetone wet paper cloth and letting it dry for 2 minutes.

In treatment T0-ref, after the first cleaning, samples were mechanically abraded with P180 sandpaper, roughening the bond area. Afterwards, they were degreased with acetone again to remove any abrasion residue. This is the most fundamental treatment used and the one used in our previous work [35]. As such, it will be used as a reference when comparing with the other ones. The failure surfaces for all the methodologies resulting from this treatment can be seen in Figure S1.

For treatment T1-deg and T2-deg-abr sheets were exposed to an alkaline degreasing solution of the following composition: 1% Na_2SiO_3, 1% Na_2CO_3, 1.5% Na_3PO_4, 0.5% SDBS. They were immersed in this solution at 80˚C for 10 minutes, washed with Mili-Q water, air-dried for 10 minutes and dried in an oven for 10 minutes at a maximum temperature of 70˚C. Treatment T2-deg-abr included mechanical abrasion before the immersion.

The aluminum sheets prepared with treatments T3-pla-5, T4-pla-5-abr and T5-pla-10-abr were exposed to atmospheric plasma using a PiezoBrush PZ3 from Relyon Plasma (Regensburg, Germany) for 5 minutes in the case of T3-pla-5 and T4-pla-5-abr and 10 minutes in the case of T5-pla-10-abr. Additionally, in samples T4-pla-5-abr and T5-pla-10-abr mechanical abrasion was conducted before plasma treatment. The sheets were used to create the joints expeditiously, as any delay could negatively impact the plasma activation of the surface. Plasma exposure was carried out with a distance of less than 1 mm between the apparatus and the aluminum sheets but ensuring no contact between the sheets and the apparatus. A 100% power setting was used in all samples and the nearfield module for electrically conductive substrates.

The exposure time was selected based on preliminary wettability tests. Different areas of an aluminum plate were exposed to atmospheric plasma for varying durations, ranging from 30 seconds to 10 minutes, including a control sample with no exposure. Immediately after treatment, a water droplet was placed on each area to visually assess changes in wettability. The plates with the different exposed areas and water droplets are shown in Figure S2. Based on these observations, exposure times of 5 and 10 minutes were chosen, as they exhibited the most significant differences in wettability.

Treatments T6-chem-NO3, T7-chem-alkUS and T8-chem-P2 involved the immersion of the sheets on different chemical etching solutions. In the case of treatment T6-chem-NO3 the immersion was done on an etching solution that contained the degreasing components as well as the etching substance (nitrate), its composition was the following: 1% Na_2SiO_3, 1% Na_2CO_3, 1.5% Na_3PO_4, 0.5% SDBS and 3% KNO_3. The sheets were exposed to this solution at 80˚C for 1.5 minutes. After this time the samples were rinsed with Mili-Q water and left to air-dry for 10 minutes before being hot-dried at a maximum temperature of 60˚C in an oven for 10 minutes. Treatment T7-chem-alkUS is based on a modified surface treatment developed by Saleema et al. [39] which consists of immersing the aluminum sheets on a 0.1M NaOH solution placed on an ultrasonic bath and sonicating them for 30 minutes before rinsing and drying them as in the other immersion methods. Finally, treatment T8-chem-P2 is based on the P2 etch procedure, a chromate-free method frequently used in industry [41]. First, the samples were degreased (such as in T1-deg and T2-deg-abr) by immersion on the degreasing solution for 10 minutes at 80˚C. After being rinsed with Mili-Q water and air-dried, they were immersed in an acid etching solution composed of 30% H_2SO_4 and 140g/L $Fe_2(SO_4)_3$ for 12 minutes at 63˚C. Afterwards, they were first thoroughly rinsed with agitated running distilled water for 2 minutes and then, with Mili-Q water for about 10 seconds to eliminate any residue from the previous step. Once the last rinse was done, the sheets were air-dried for 10 minutes at room temperature and 15 minutes at a maximum temperature of 70˚C. Some images of these procedures can be found in Figure S3.

In treatments T1-deg, T2-deg-abr, T6-chem-NO3, T7-chem-alkUS, and T8-chem-P2 the treated aluminum sheets were used as soon as possible, with a maximum of 4 hours between treatment and bonding. In the case of treatments T3-pla-5, T4-pla-5-abr, and T5-pla-10-abr less than 30 minutes went by between treatment and bonding. Due to the highly reactive nature of plasma modification, it was crucial to handle exposed samples with haste.

2.4 Single-lap joint assembly

Four different methodologies were used to test the joints: testing of pristine adhesion, testing the re-adhesion after break, the re-adhesion after debonding and the adhesion after self-welding. To test pristine adhesion, the vitrimer adhesive was applied in the overlapping region of 12.5 mm between two sheets of aluminum provided with Teflon spacers to ensure an adequate and uniform bond-line thickness of 1.0 mm. After adhesive application, the joints were cured in an oven at the temperatures and times specified in Section 2.2 while applying a constant pressure of 4.8 KPa.

In order to prepare the samples for the testing of the re-adhesion methodologies, the dynamic nature of the vitrimer was exploited. At a temperature of 180˚C, the adhesive undergoes rapid stress relaxation, allowing the joints to be reprocessed. To produce the adhesion after break test samples, the two halves of a joint that had been tested to failure for pristine adhesion (as described in Section 2.5) were brought together under a pressure of 8 MPa, to ensure good contact, and after 2 hours at 180˚C the joint was recovered and ready for tensile testing. For the adhesion after debonding, an untested joint is heated, using

the same conditions (2h at 180˚C), and due to the relaxation mechanism being active at this temperature, the sample can be disassembled manually. Afterwards, it is reassembled by applying the re-adhesion conditions (8Mpa and 2h at 180˚C) to reform the bond. Finally, for the adhesion after self-welding samples, two aluminum sheets were independently coated with the vitrimer adhesive with a thickness that was half the desired bond-line (0.5 mm) and cured separately under a constant pressure of 4.8 KPa. The final joint to be tested was then obtained by pressing the two coated sheets together and applying the same re-adhesion conditions (180˚C, 2 h, 8 MPa) allowing the adhesive to form a continuous bond due to the vitrimeric network reorganization.

2.5 Lap shear strength quantification

The lap shear strength of all the single-lap joints prepared as specified in Section 2.4 was evaluated by tensile lap shear tests according to the UNE-EN ISO 1465:2009 standard [42]. A universal testing machine Lloyd EZ50 (Bognor Regis, UK) was used equipped with a 50 kN load cell and at 1.3 mm/min crosshead speed. At least five samples were tested in each experiment, and the average lap-shear stress was calculated. The determination of the type of failure was done, in all cases, through visual inspection following the guidelines from standard UNE-EN ISO 10365:2022 [43].

2.6 Statistical analyses of the effect of the different superficial treatments

Due to the high dispersion of the results obtained in the lap-shear tests, statistical analyses were conducted in order to have a robust methodology to elucidate which treatments had a significant impact on the adhesion and re-adhesion performances.

To assess group differences while accounting for unequal variances, the initial test performed was Brown-Forsythe. This test revealed statistically significant differences in variances between the treatment groups. Consequently, Welch's one-way ANOVA was employed to compare the means among each treatment group. Additionally, the Benjamini-Hochberg (B-H) procedure was implemented to control the false discovery rate when conducting multiple comparisons to make sure that true effects were discovered. The confidence level was set at 95% (α=0.05) for all tests.

In Tables S1 to S4 of the Supporting Information, the comparisons that were deemed interesting to perform are shown, as well as their p values, B-H critical values, and whether they passed the p test and the B-H correction.

2.7 Aluminum surface characterization

To characterize the surfaces, contact angle measurements were performed using an OCA 15EC goniometer (DataPhysics Instruments USA Corp, Charlotte, NC, USA) on aluminum sheets samples immediately after the treatments were applied. A droplet of Mili-Q water was deposited onto the surface and, using a video camera, the contact angle was calculated after 30 seconds for 5 different samples using the SCA software provided in the apparatus. Field emission sweeping electron microscopy (FESEM) was performed on a Scios 2 Dual Beam from Thermo Fischer Scientific (Waltham, MA, USA) on samples just after the treatments were applied and after failure of the joints, in order to understand the adhesive-surface interaction that leads to re-adhesion. Additionally, energy-dispersive X-ray spectroscopy (EDS) was conducted during FESEM analysis to perform a microanalysis of the elemental composition of the surfaces before treatment, providing further insight into possible chemical changes affecting adhesion.

3. Results and discussion

Table 2 shows the adhesion and re-adhesion values for the samples with each superficial treatment and for each adhesion methodology with a bond-line thickness of 1.0 mm. The force-displacement curves of all the lap-shear tests can be found in Figure S5 to S13.

All nine treatments evaluated were tested for pristine adhesion and re-adhesion after break. In the case of the other two re-adhesion methodologies (re-adhesion after debonding and adhesion after self-welding), only the treatments that presented more promising results were evaluated. Treatment T2-deg-abr was chosen over T1-deg as the mean value is higher for pristine adhesion and no significant differences were present in re-adhesion after break. In the case of plasma treatments, T4-pla-5-abr was chosen over T3-pla-5 and T5-pla-10-abr as it was the only one that showed improvement in re-adhesion after break. Lastly, all chemical etching treatments were maintained as each one was observed to have promising results: Treatment T6-chem-NO3 showed one of the highest mean values for pristine adhesion, and treatments T7-chem-alkUS and T8-chem-P2 presented the highest re-adhesion after break mean values. These six treatments were also analyzed by water contact angle and FESEM microscopy, in order to study their wettability and surface morphology and composition (see Table 3, Figures 2 and Figure 3).

Figure 1 shows a dispersion graph of the lap shear test results obtained with each methodology, for comparative purposes. At first glance, it can be seen that the results present a high dispersion of values. For this reason, in order to have an objective procedure to ascertain which treatments induced a substantial change in adhesion strength, statistical analyses were performed, as exposed in Section 2.6. In Tables S1, S2, S3 and S4 of the supporting information the statistical parameters are shown and the comparisons that showed a statistically significant difference are highlighted.

Table 2. Adhesion strength values from lap-shear tests of each treatment with the four different adhesion methodologies. For the re-adhesion methodologies the percentage of the mean respect to the mean of pristine adhesion (the adhesion retention) of each treatment is also shown. Horizontal rules are used to distinguish between treatment categories.

Sample	Pristine adhesion (MPa)	Re-adhesion after break (MPa)	Re-adhesion after debonding (MPa)	Adhesion after self-welding (MPa)
T0-ref [35]	12.6 ± 1.9	7.0 ± 0.8 (55%)	11.4 ± 3.9 (90%)	5.5 ± 2.4 (44%)
T1-deg	18.4 ± 4.8	8.2 ± 8.5 (45%)	-	-
T2-deg-abr	23.9 ± 8.5	5.9 ± 3.1 (25%)	16.2 ± 1.8 (68%)	10.4 ± 1.1 (44%)
T3-pla-5	13.9 ± 1.2	7.3 ± 4.1 (53%)	-	-
T4-pla-5-abr	15.3 ± 2.9	10.3 ± 1.9 (67%)	11.2 ± 4.0 (73%)	12.1 ± 3.4 (79%)
T5-pla-10-abr	13.7 ± 6.8	4.2 ± 1.6 (31%)	-	-
T6-chem-NO3	22.4 ± 3.6	10.8 ± 4.0 (48%)	14.7 ± 2.1 (66%)	5.3 ± 3.1 (24%)
T7-chem-alkUS	15.9 ± 1.7	12.0 ± 3.0 (75%)	14.8 ± 3.0 (93%)	12.6 ± 2.5 (79%)
T8-chem-P2	15.1 ± 1.6	12.8 ± 2.5 (85%)	16.3 ± 2.9 (108%)	10.5 ± 3.4 (70%)

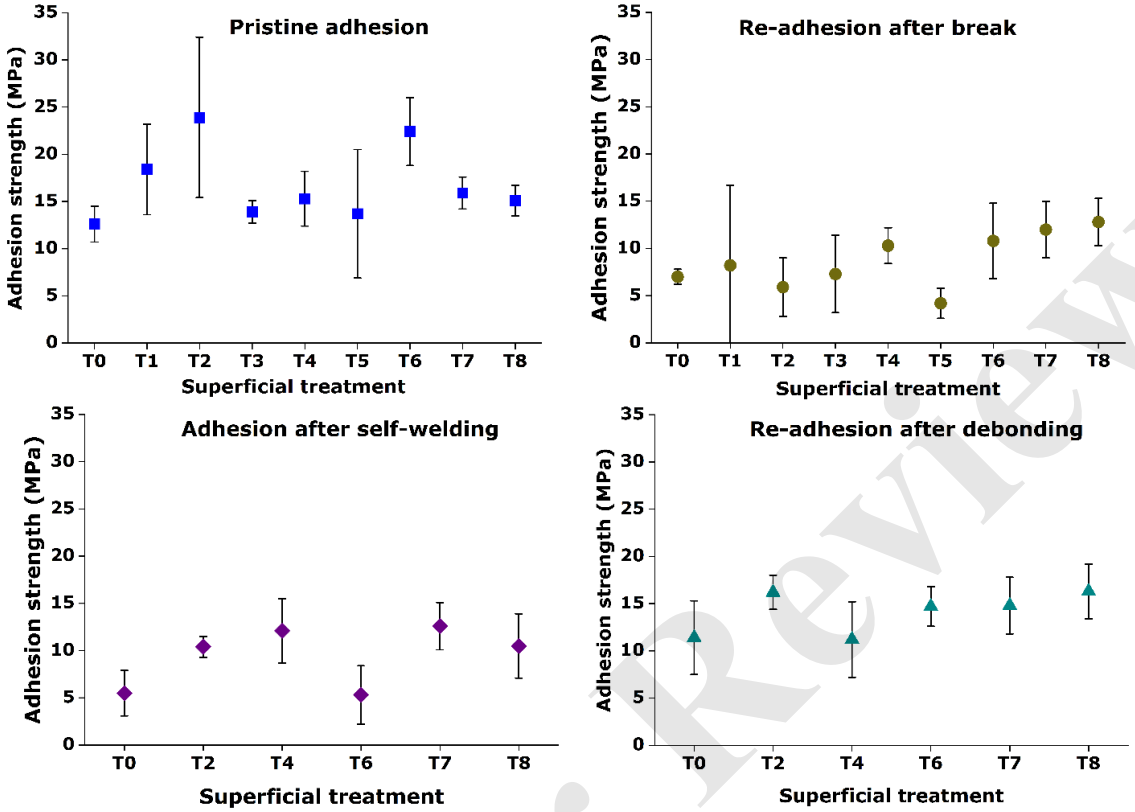

Figure 1. Dispersion graphs of the different lap shear stress values obtained for all methodologies on each treatment.

The following sections provide a detailed analysis of the effect of each treatment on the different adhesion methodologies individually, followed by an assessment of their impact across all methodologies.

3.1 Pristine adhesion

The data in Table 2 shows that the mean lap-shear stress values for pristine adhesion are higher for all treatments performed (T1-deg to T8-chem-P2) when compared to the reference treatment T0-ref, as expected. Treatments T1-deg and T2-deg-abr show an enormous increase in lap shear stress compared to T0-ref, particularly T2-deg-abr with a very substantial 90% increment. In other similar studies focused on pristine adhesion, an alkaline degreasing method only caused around a 30% increment [44]. This is possibly because in those studies the control sample has a more complex treatment than T0-ref, but highlights the substantial effect of the degreasing treatment. This striking improvement can also be identified through surface analysis. In Table 3, the apparent water contact angle of the aluminum surface after each treatment can be seen, and it shows that sample T2-deg-abr shows an incredibly low value of water contact angle, of only 13.4°, due to the elimination of contaminants. In Figure 2, FESEM micrographs of the adherents' surface after different treatments can be seen and comparing T0-ref (Figure 2 a) and b)) and T2-deg-abr (Figure 2 c) and d)) it becomes evident that all foreign matter or particles are eliminated

while the overall topography stays constant. Furthermore, microanalysis (Table S5) shows much less C and O content.

When comparing the two different degreasing treatments used (T1-deg and T2-deg-abr), both lap shear stress values are not statistically significantly different. This suggests a negligible effect of mechanical abrasion on adhesion strength for this pair, as that was the only differentiating feature of these two treatments.

Although treatments T3-pla-5, T4-pla-5-abr and T5-pla-10-abr show a higher mean value than that of T0-ref, they do not show a statistically significant difference with respect to treatment T0-ref, as evidenced by the statistical parameters shown in Table S1. This is in discordance with other works where they used atmospheric plasma jets as a superficial treatment for adhesive bonding [36–38,45], where substantial improvements were found for lap-shear strength. Additionally, some studies [46,47] demonstrated that the exposure of aluminum alloys to atmospheric plasma modifies the passive oxide layer present and converts it to aluminum oxyhydroxide and aluminum hydroxide, with the amount of conversion being related to the time of exposure. In this work, the exposure times of 5 and 10 minutes were selected based on preliminary wettability tests, which showed significant differences in surface hydrophilicity depending on treatment duration (see section 2.3 and Figure S2). To corroborate this, results from contact angle goniometry experiments were analyzed. This conversion can be inferred from the change in wettability (see Table 3), with a shift to hydrophilicity shown by a decrease in an apparent water contact angle from 88.9˚ for T0-ref to 45.3˚ for T4-pla-5-abr. This is possibly due to the presence of hydroxide groups in the newly formed coating, which interact favorably with water molecules. Nevertheless, these hydroxide-containing substances are mechanically weaker than the original oxide layer. In light of these observations, it is possible that the conditions used in this work, especially an exposure time too prolonged, lead to an excessive conversion which, in turn, results in this layer acting as a weak boundary layer that does not favor a high lap-shear stress for the samples exposed to plasma in this work. Furthermore, it creates inconsistencies in the re-adhesion methodologies results.

As for chemical etching treatments, T7-chem-alkUS and T8-chem-P2 show statistically the same value which is a moderate increase of around 20-25%. For T7-chem-alkUS this is not as high as the 50% increase shown by Saleema et al. with this treatment[39], probably due to the different alloys used. Nevertheless, it is a substantial improvement. For T8-chem-P2 the increase is in line with other works with similar treatment [44]. By contrast, treatment T6-chem-NO3 exhibits the second highest lap-shear stress value, it represents a striking improvement of 77%.

This adhesion behavior of the chemical etching treatments is also reflected in the surface characteristics analyzed. All three chemical treatment sample surfaces show extremely hydrophilic character in contact angle measurements, 22.9˚ for T6-chem-NO3, 23.9˚ for T7-chem-alkUS and 8.3˚ for T8-chem-P2, as seen in Table 3. In Figure 2 e) and f) the micrographs of the T6-chem-NO3 surface can be seen. At low magnification, the surface of sample T6-chem-NO3 does not seem to present etching effects. When observed at a higher magnification, however, the effect of the chemical etching treatment can be appreciated. The nitrate oxidizing agent has attacked the surface, leaving behind irregular etch pits with sharp edges and dimensions of approximately 200 nm. These pits increase the surface contact between adhesive and adherent and act as anchoring sites for the adhesive, allowing for such high lap shear stress. In the case of T7-chem-alkUS (Figure 2 g) and h)) and T8-chem-P2 (Figure 2 i) and j)) the effect is much more evident at lower magnifications, showing regular and defined microstructures. In sample T7-chem-alkUS, at lower

magnifications, some big etch pits can be seen and the grain boundaries seem to be exposed. Furthermore, the surface overall presents shallow concave pits. Further magnification reveals a really textured structure, contributing to more microroughness. In the case of samples T8-chem-P2, at higher magnification a patterned texture is revealed, a cellular sponge-like structure of holes and cavities. Undoubtedly, this textured surface together with the decrease on water contact angle are responsible for the increase in lap-shear strength of the samples. However, T6-chem-NO3 has a substantially higher increase, which indicates that the smaller but deeper cavities are more effective mechanical locks for the adhesive.

Interestingly, regardless of the overall higher mean values for pristine adhesion, all pristine adhesion samples independent of treatment show an adhesive failure, as seen in Figure S14.

Table 3. Apparent water contact angle found for the aluminum adherents after each superficial treatment.

Treatment	T0-ref	T2-deg-abr	T4-pla-5-abr	T6-chem-NO3	T7-chem-alkUS	T8-chem-P2
Apparent water contact angle (˚)	88.9	13.4	45.3	22.9	23.9	8.3

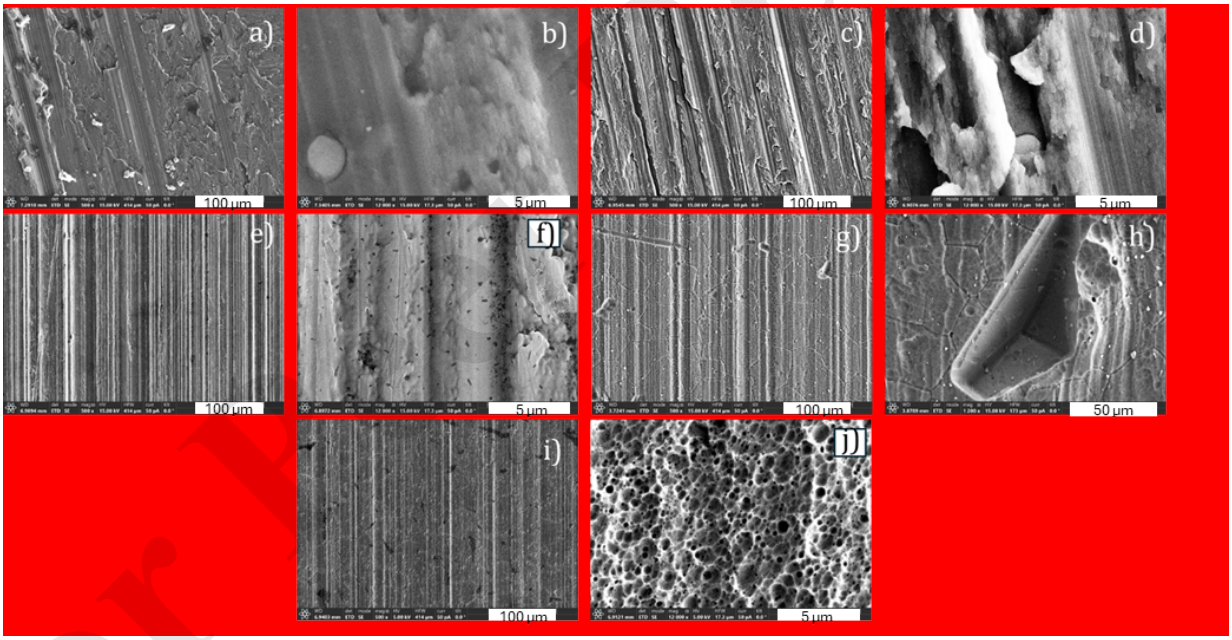

Figure 2. SEM micrographs of the aluminum adherents after each treatment. T0-ref (a and b), T2-deg-abr (c and d), T6-chem-NO3 (e and f), T7-chem-alkUS (g and h) and T8-chem-P2 (i and j). Micrographs a), c), e), g), and i) were taken at 500x magnification, micrograph h) at 1200x and micrographs b), d), f) and j) at 12000x.

3.2 Re-adhesion after break

Values for re-adhesion after break are not straightforward to analyze due to the inherent challenge of perfectly aligning both aluminum halves after the lap-shear test, ensuring a perfect fit between their respective adhesive remains. Furthermore, aluminum adherents have a relatively low yield strength, which leads to plastic deformation at high lap-shear

stress values that drastically impair re-adhesion, as we have reported before [35,48]. A trivial solution to this issue is the use of thicker aluminum plates, but in order to stay within the parameters of the UNE-EN ISO 1465:2009 standard all adherents tested had a thickness of 2.0 mm. Additionally, adherent thickness is not a parameter that can usually be changed in the assembling process at the industrial scale and it can also influence adhesion strength. Despite these challenges, this methodology was included in the present work as most literature written about reversible adhesives focuses on this re-adhesion mode [10,13,15,17,19], including the work of Wu et al. [30] on the anodization of aluminum alloy to enhance vitrimer re-adhesion.

Considering the statistical treatment of the data, summarized in Table S2, the only samples that show statistically significant differences to T0-ref are treatments T4-pla-5-abr, T5-pla-10-abr, T7-chem-alkUS and T8-chem-P2. The fact that the treatments that showed the highest lap-shear stress in pristine adhesion (T1-deg, T2-deg-abr and T6-chem-NO3) do not show any improvement in re-adhesion after break can be attributed to the plastic deformation of the adherents, as mentioned above, which in the authors' experience is critical above 16MPa of shear stress with the specified dimensions. The plasma samples (T3-pla-5, T4-pla-5-abr and T5-pla-10-abr) show inconsistent results, which as exposed above, are probably due to the new oxide layer formed acting as a weak boundary layer.

Treatment T7-chem-alkUS and T8-chem-P2 show no significant differences among them and they both demonstrate a great re-adhesion improvement compared to T0-ref. This improvement is shown by a value of re-adhesion after break 75% higher than that of T0-ref, which represents an 80% retention of their original pristine adhesion strength. This is due to an effective surface modification (as seen by pristine adhesion results and morphology and wettability of the surfaces (see Table 3 and Figure 2)) and a pristine adhesion lap-shear value that is moderate enough to not cause severe plastic deformation on the aluminum adherents.

3.3 Re-adhesion after debonding

The results from Table 2 reveal that all mean values of re-adhesion after debonding, except for T4-pla-5-abr, are higher than T0-ref. However, the statistical analysis from Table S3 reveals that no surface treatment had a significant impact on re-adhesion after debonding when compared to T0-ref. Notwithstanding, a closer look at the mean values for each treatment might provide valuable insights, particularly in comparison to the other methodologies employed. For instance, treatments T2-deg-abr and T8-chem-P2 exhibited trends towards significance, with a low p-value, but did not remain statistically significant after applying the Benjamini-Hochberg correction for multiple comparisons (Table S3). Nevertheless, these samples were the ones to attain the most substantial increase, showing a lap-shear stress value 43% higher than that of T0-ref. For T2-deg-abr, this represents 68% of its pristine adhesion and for T8-chem-P2, a striking 108%.

These results suggest that re-adhesion after debonding is only moderately affected by surface preparation. In this methodology, the adhesive joints are dismantled using minimal force (with bare hands), because of this, the adhesive-aluminum interactive forces are not surpassed, and a cohesive failure mode is obtained as confirmed by the pictures in Figure S15. This would logically be the critical step in this methodology, which affords the best re-adhesion results thanks to the low stress required to dismantle the joint. In turn, this low stress granted by the ability of the vitrimer to relax stresses at the processing temperature, renders the re-adhesion after debonding values mostly independent of the treatment used, as the adhesive-aluminum interaction can hardly be surpassed at this stage.

The failure surfaces of these samples after testing can be found on Figure S16.

3.4 Adhesion after self-welding

Of the treatments tested for this methodology, the only one that did not reach a statistically significant difference when compared to T0-ref is treatment T6-chem-NO3, as seen in Table S4; this is reflected in their similar mean values. All the other values represent a significant improvement compared to T0-ref. In fact, this methodology seems to be the most influenced by surface preparation, as the most considerable improvements are found here. This significant improvement is further corroborated by the failure mode, as shown in Figure S17, which exhibits the most cohesive contributions across all samples. In our previous work [35], we studied the influence of bond-line thickness on the re-adhesion of this vitrimer adhesive. There, we demonstrated that when the bond-line increased, so did the cohesive forces inside the vitrimer, as there are more reaction partners available. Because of this, with untreated aluminum adherents the adhesive forces are easily surpassed by the cohesive ones. In the current case, however, with greatly reinforced adhesion forces coming from the treated surfaces, the joint is able to sustain higher lap-shear stress, which justifies the overall higher values for this methodology.

Figure 3 shows the SEM micrographs of the aluminum samples taken after the lap-shear test. These micrographs show how the texture of the adherent helped the adhesive adhere and are very helpful when interpreting re-adhesion results.

Treatment T2-deg-abr presents a mean value that is 89% bigger than that of T0-ref with a very low uncertainty. The lap-shear strength attained represents only 44% of its original adhesion strength because of the high value achieved for pristine adhesion. In Figure 3 a), b) and c) the micrographs of T0-ref can be seen. In a general sense, at the lowest magnification, the surface of T0-ref is the one that seems to have the least amount of adhesive remains. The remains seem to be relatively big chunks of the polymer, which at higher magnification can clearly be seen to be immobilized between ridges or under flakes (which is, indeed, the only roughness source on those surfaces). The surface of treatment T2-deg-abr (Figure 3 d) and e)) seems to have a bit more adhesive material on it, and while a portion is also stuck in the valleys between ridges, there is much more material adhered to areas without this kind of roughness. It is rational to think that this is due to the higher surface cleanliness and wettability, which affords a higher adhesive bond in areas where mechanical interlocking is not possible. This can be the reason for the higher adhesion and re-adhesion (after debonding and after self-welding) performance of this treatment.

Treatment T4-pla-5-abr, exhibits a high increase of 120% respect to T0-ref, which represents a 79% retention of pristine adhesion. This increment contradicts the trend observed for the other plasma treatments and methodologies, and further emphasizes the importance of optimizing plasma exposure parameters, as excessive treatment times may negatively impact adhesion.

Treatment T6-chem-NO3, as previously stated, does not present an improvement compared to T0-ref. This is also unexpected, as the mean values in the other three methodologies were higher than the T0-ref reference. The micrographs of the samples with this treatment can be found in Figure 3 f) and g). Observing these micrographs, the etching pits produced by the treatment, which act as mechanical locks for the adhesive, can be seen to be totally covered by the adhesive after failure of the joint. In fact, these are the only areas where adhesive is found in these samples after failure, offering a relatively low surface area for the self-welding process. Due to this, the pristine adhesion of this sample is one of the highest,

but re-adhesion performance is relatively poor. This is a relevant conclusion, as it demonstrates that not all treatments known to improve adhesion strength will increase re-adhesion performance.

Finally, treatments T7-chem-alkUS and T8-chem-P2 show substantial improvement compared to the reference. They show an improvement of up to 130% (for the mean value of T7-chem-alkUS) and a retention of its original adhesion strength of around 75%. The micrographs for T7-chem-alkUS are found in Figure 3 h) and i). They reveal that this is the sample with the most adhesive remains on the surface, a thick coating of adhesive can be seen over most of the surface. This, combined with a low contact angle, easily explains the good re-adhesion performance of the samples. Treatment T8-chem-P2 (Figure 3 j) and k)) at low magnification, shows a similar scenario to treatment T0-ref, with big pieces of adhesive around ridges and other roughness of the surface. However, higher magnifications reveal that the adhesive is greatly anchored on the sponge-like structure, which enhances the surface area coated with adhesive that is available for the self-welding mechanism and that is responsible for the improved re-adhesion performance of the treated joints.

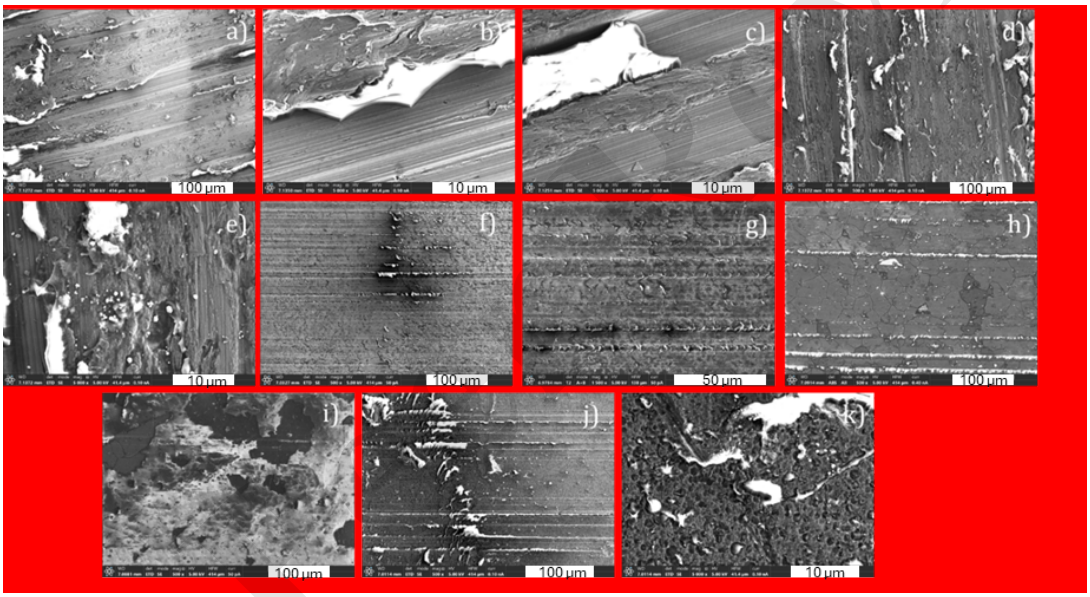

Figure 3. SEM micrographs of the treated aluminum adherents after failure of the adhesive joint for the adhesion after self-welding. T0-ref (a, b and c), T2-deg-abr (d and e), T6-chem-NO3 (f and g), T7-chem-alkUS (h and i) and T8-chem-P2 (j and k). Micrographs a), d), f), h), i) and j) were taken at 500x magnification, g) at 1500x and b), c), e) and k) at 5000x.

3.5 Discussion of superficial treatments across methodologies

Evaluating each treatment within individual methodologies provided insight into the adhesive mechanisms governing each adhesive application. Shifting the focus on performance across methodologies elucidates the most effective treatment overall.

Treatments T7-chem-alkUS and T8-chem-P2 showed a higher lap-shear stress value than T0-ref in all methodologies. Treatment T2-deg-abr significantly improves the mean values of pristine adhesion, re-adhesion after debonding and adhesion after self-welding compared to T0-ref. The only methodology that does not experiment an improvement is re-adhesion

after break, which, as already mentioned, can be explained by the plastic deformation of the aluminum adherents.

Treatment T6-chem-NO3 exhibited the highest mean value of pristine adhesion strength of all treatments, with relatively low dispersion. Nevertheless, all re-adhesion methodologies with this treatment showed no significant differences compared to T0-ref. Curiously, this seems to indicate that the nitrate etch used in this work only affects original adhesion, while re-adhesion remained unaffected. As said before, it seems that not all treatments that are known to improve adhesion influence re-adhesion the same way.

Finally, treatments T7-chem-alkUS and T8-chem-P2 displayed significant improvements compared to T0-ref across all adhesion tests. Pristine adhesion increased by 25%, while re-adhesion after break and self-welding saw a remarkable 75% and 100% increase, respectively. Notably, both treatments achieved near-perfect retention (almost 100%) of their original adhesion after debonding, with T8-chem-P2 nearing a statistically significant difference from the reference treatment.

In light of these results, treatments T2-deg-abr, T7-chem-alkUS and T8-chem-P2 emerge as effective solutions for improving the re-adhesion strength of reversible vitrimeric adhesive systems when used with aluminum adherents.

4. Conclusions

Our findings provide compelling evidence that superficial treatment significantly influences re-adhesion performance of vitrimer adhesives. This work emphasizes the importance of the substrate's surface characteristics, in addition to the intrinsic properties of the adhesive itself. Re-adhesion, as demonstrated here, is a complex phenomenon governed by the interplay between the adhesive's chemistry, the mechanics of failure/dismantling, and the bond formed between the adhesive and the adherent. Furthermore, by using a vitrimeric adhesive, different re-adhesion methodologies could be studied, and not all of them were affected the same way by the surface treatments.

The different effects of the treatments were quantified in terms of adhesion strength, and the surfaces were also studied using contact angle measurements and FESEM microscopy, which led to a further understanding of the mechanics of re-adhesion.

While some questions are left unanswered, particularly regarding the best conditions to be used for atmospheric plasma exposure, the results derived from this work shine the spotlight on the positive effects that surface treatment technology can have on the reversible adhesion of vitrimer adhesives. These conclusions can be potentially extended to other kinds of reversible adhesives as well. Treatments T2-deg-abr, T7-chem-alkUS and T8-chem-P2 are great options to enhance reversible adhesion on aluminum adherents without changing the adhesive chemistry or properties. For this reason, we encourage researchers in this field to, whenever possible, consider using a similar approach in order to improve re-adhesion performance and push reversible adhesives towards wider adoption.

Corresponding author

david.santiago@eurecat.org

silvia.delaflor@urv.cat

Funding details

This work is part of the R&D projects projects PID2023-147128OB-C22 and TED2021-131102B-C22 funded by MCNI/AEI/10.13039/501100011033, European Union NextGenerationEU"/PRTR, and ACCIÓ-Eurecat (Project Flagship – Intelligent). We acknowledge these grants and the Generalitat de Catalunya (2021-SGR-00154). Marc Surós is a fellow of Eurecat's "Vicente López" grant program.

Disclosure statement

The authors report there are no competing interests to declare.

Data availability statement

The authors confirm that the data supporting the findings of this study are available within the article and its supplementary materials.

References

[1] M.Q. dos Reis, M.D. Banea, L.F.M. da Silva, R.J.C. Carbas, Mechanical characterization of a modern epoxy adhesive for automotive industry, Journal of the Brazilian Society of Mechanical Sciences and Engineering 41 (2019). https://doi.org/10.1007/s40430-019-1844-2.

[2] Antonio Pizzi, K.L. Mittal, Handbook of Adhesive Technology, Third Edition, CRC Press, 2017. https://doi.org/10.1201/9781315120942.

[3] Motor vehicle production growth worldwide | Statista, (2024). https://www.statista.com/statistics/1097267/worldwide-motor-vehicle-production-growth/ (accessed May 20, 2024).

[4] L.A. López Ruiz, X. Roca Ramón, S. Gassó Domingo, The circular economy in the construction and demolition waste sector – A review and an integrative model approach, J Clean Prod 248 (2020) 119238. https://doi.org/10.1016/J.JCLEPRO.2019.119238.

[5] K.R. Mulcahy, A.F.R. Kilpatrick, G.D.J. Harper, A. Walton, A.P. Abbott, Debondable adhesives and their use in recycling, Green Chemistry 24 (2022) 36–61. https://doi.org/10.1039/d1gc03306a.

[6] A. Hutchinson, Y. Liu, Y. Lu, Overview of disbonding technologies for adhesive bonded joints, J Adhes 93 (2017) 737–755. https://doi.org/10.1080/00218464.2016.1237876.

[7] V. Silveira, R. Papadakis, S. Adamopoulos, Towards starch-based adhesives involving carbon dots as versatile crosslinkers, Journal of Adhesion (2025). https://doi.org/10.1080/00218464.2025.2464051;WGROUP:STRING:PUBLICATION.

[8] W. Denissen, J.M. Winne, F.E. Du Prez, Vitrimers: Permanent organic networks with glass-like fluidity, Chem Sci 7 (2016) 30–38. https://doi.org/10.1039/c5sc02223a.

[9] D. Montarnal, M. Capelot, F. Tournilhac, L. Leibler, Silica-Like Malleable Materials from Permanent Organic Networks, Science (1979) 334 (2011) 965–968. https://doi.org/10.1126/science.1212648.

[10] J. Tang, L. Wan, Y. Zhou, H. Pan, F. Huang, Strong and efficient self-healing adhesives based on dynamic quaternization cross-links, J. Mater. Chem. A 5 (2017) 21169–21177. https://doi.org/10.1039/C7TA06650C.

[11] J. Zheng, Z.M. Png, S.H. Ng, G.X. Tham, E. Ye, S.S. Goh, X.J. Loh, Z. Li, Vitrimers: Current research trends and their emerging applications, Materials Today 51 (2021) 586–625. https://doi.org/10.1016/j.mattod.2021.07.003.

[12] S. Zhang, T. Liu, C. Hao, L. Wang, J. Han, H. Liu, J. Zhang, Preparation of a lignin-based vitrimer material and its potential use for recoverable adhesives, Green Chemistry 20 (2018) 2995–3000. https://doi.org/10.1039/c8gc01299g.

[13] S. Zhao, M.M. Abu-Omar, Catechol-Mediated Glycidylation toward Epoxy Vitrimers/Polymers with Tunable Properties, Macromolecules 52 (2019) 3646–3654. https://doi.org/10.1021/acs.macromol.9b00334.

[14] D. Santiago, D. Guzmán, J. Padilla, P. Verdugo, S. De la Flor, À. Serra, Recyclable and Reprocessable Epoxy Vitrimer Adhesives, ACS Appl Polym Mater 5 (2023) 2006–2015. https://doi.org/10.1021/acsapm.2c02063.

[15] J. Liu, X. Liu, X. Cui, J. Qin, M. Shi, D. Wang, L. Liang, C. Yang, Imine-Containing Epoxy Vitrimer Cured by Active Ester: Properties and Theoretical Analysis, ACS Appl Polym Mater 5 (2023) 10042–10052. https://doi.org/10.1021/acsapm.3c01917.

[16] Y. Sun, M. Wang, Z. Wang, Y. Mao, L. Jin, K. Zhang, Y. Xia, H. Gao, Amine-Cured Glycidyl Esters as Dual Dynamic Epoxy Vitrimers, Macromolecules 55 (2022) 523–534. https://doi.org/10.1021/acs.macromol.1c01914.

[17] W. Yang, Q. Yi, F. Liu, X. Pan, Y. Zeng, Fabrication of malleable, repairable, weldable, recyclable and robust epoxy vitrimers from itaconic acid for recycled adhesion, Eur Polym J 196 (2023). https://doi.org/10.1016/j.eurpolymj.2023.112278.

[18] Y. Yang, H. Zhou, X. Chen, T. Liu, Y. Zheng, L. Dai, C. Si, Green and ultrastrong polyphenol lignin-based vitrimer adhesive with photothermal conversion property, wide temperature adaptability, and solvent resistance, Chemical Engineering Journal 477 (2023). https://doi.org/10.1016/j.cej.2023.147216.

[19] Z. Zhou, X. Su, J. Liu, R. Liu, Synthesis of Vanillin-Based Polyimine Vitrimers with Excellent Reprocessability, Fast Chemical Degradability, and Adhesion, ACS Appl Polym Mater 2 (2020) 5716–5725. https://doi.org/10.1021/acsapm.0c01008.

[20] H. Gao, X. Wu, J. Fan, Z. Wang, Mechanically Strong and Tough Plant Oil-Based Poly(ester amide) Vitrimers with Closed-Loop Recyclability, ACS Sustain Chem Eng 12 (2024) 2668–2677. https://doi.org/10.1021/acssuschemeng.3c06783.

[21] J. Wu, X. Yu, H. Zhang, J. Guo, J. Hu, M.-H. Li, Fully Biobased Vitrimers from Glycyrrhizic Acid and Soybean Oil for Self-Healing, Shape Memory, Weldable, and Recyclable Materials, ACS Sustain Chem Eng 8 (2020) 6479–6487. https://doi.org/10.1021/acssuschemeng.0c01047.

[22] A. Moreno, M. Morsali, M.H. Sipponen, Catalyst-Free Synthesis of Lignin Vitrimers with Tunable Mechanical Properties: Circular Polymers and Recoverable Adhesives, ACS Appl Mater Interfaces 13 (2021) 57952–57961. https://doi.org/10.1021/acsami.1c17412.

[23] Z. Luo, X. Pan, F. Liu, Q. Yi, Y. Zeng, Y. Chen, C. Wang, Catalyst-free epoxy vitrimers from rosin: Highly mechanical performance, fast self-healing, and facile recycling, Eur Polym J 202 (2024). https://doi.org/10.1016/j.eurpolymj.2023.112606.

[24] A. Trejo-Machin, L. Puchot, P. Verge, A cardanol-based polybenzoxazine vitrimer: Recycling, reshaping and reversible adhesion, Polym Chem 11 (2020) 7026–7034. https://doi.org/10.1039/d0py01239d.

[25] C. Li, Y. Chen, Y. Zeng, Y. Wu, W. Liu, R. Qiu, Strong and recyclable soybean oil-based epoxy adhesives based on dynamic borate, Eur Polym J 162 (2022). https://doi.org/10.1016/j.eurpolymj.2021.110923.

[26] P. Li, J. Zhang, J. Ma, C.A. Xu, X. Liang, T. Yuan, Y. Hu, Z. Yang, Fully bio-based thermosetting polyimine vitrimers with excellent adhesion, rapid self-healing, multi-recyclability and antibacterial ability, Ind Crops Prod 204 (2023). https://doi.org/10.1016/j.indcrop.2023.117288.

[27] H.H. Moon, I. Cha, H.A. Hegazy, K. su Kim, C. Song, Covalent adaptive polymer networks for switchable adhesives, Bull Korean Chem Soc 44 (2023) 750–767. https://doi.org/10.1002/bkcs.12722.

[28] A. Roig, L. Molina, À. Serra, D. Santiago, S. De la Flor, Structural reversible adhesives based on thiol-epoxy vitrimers, Polym Test 128 (2023). https://doi.org/10.1016/j.polymertesting.2023.108205.

[29] L. Li, X. Chen, J.M. Torkelson, Covalent Adaptive Networks for Enhanced Adhesion: Exploiting Disulfide Dynamic Chemistry and Annealing during Application, ACS Appl Polym Mater 2 (2020) 4658–4665. https://doi.org/10.1021/acsapm.0c00720.

[30] Z. Wu, Y. Zhao, W. Guo, Q. Zhang, G. Wang, C. Gao, Strengthening epoxy vitrimer/Al alloy interfaces: Anodization as a key to enhanced adhesion, Mater Lett 384 (2025). https://doi.org/10.1016/j.matlet.2025.138073.

[31] F. Awaja, M. Gilbert, G. Kelly, B. Fox, P.J. Pigram, Adhesion of polymers, Progress in Polymer Science (Oxford) 34 (2009) 948–968. https://doi.org/10.1016/j.progpolymsci.2009.04.007.

[32] S. Ebnesajjad, A.H. Landrock, Adhesives Technology Handbook, Elsevier, 2015. https://doi.org/10.1016/C2013-0-18392-4.

[33] Anna Rudawska, Surface Treatment in Bonding Technology, Elsevier, 2019. https://doi.org/10.1016/C2018-0-01281-5.

[34] B. Özakin, K. Gültekin, Synergetic effect of hybrid surface treatment on the mechanical properties of adhesively bonded AA2024-T3 joints, Journal of Adhesion (2024). https://doi.org/10.1080/00218464.2024.2412714.

[35] M. Surós, D. Santiago, P. Verdugo, M. Pedrola, S. De la Flor, Reversible adhesives from epoxy-based transesterification-induced vitrimers, Polymer (Guildf) 299 (2024). https://doi.org/10.1016/j.polymer.2024.126939.

[36] D. Ba, Q. Qiao, C. Li, H. Cui, H. Zhang, Low-Temperature Plasma Treatment of Aluminum for Improved Surface Bonding, J Mater Eng Perform 33 (2024) 1816–1826. https://doi.org/10.1007/s11665-023-08082-2.

[37] M.A. Castillo Acero, L.C. López, Effect of plasma treatment in Aluminum and composites bonding joints: Shear load tests results, Procedia Manuf 13 (2017) 183–189. https://doi.org/10.1016/j.promfg.2017.09.034.

[38] T.S.M. Mui, L.L.G. Silva, V. Prysiazhnyi, K.G. Kostov, Surface modification of aluminium alloys by atmospheric pressure plasma treatments for enhancement of their adhesion properties, Surf Coat Technol 312 (2017) 32–36. https://doi.org/10.1016/j.surfcoat.2016.08.024.

[39] N. Saleema, D.K. Sarkar, R.W. Paynter, D. Gallant, M. Eskandarian, A simple surface treatment and characterization of AA 6061 aluminum alloy surface for adhesive bonding applications, Appl Surf Sci 261 (2012) 742–748. https://doi.org/10.1016/j.apsusc.2012.08.091.

[40] Structural Adhesives Guidelines for surface preparation of metals and plastics prior to adhesive bonding @, 2004. www.une.org.

[41] A.N. Rider, D.R. Arnott, J.J. Mazza, Surface Treatment and Repair Bonding, in: Aircraft Sustainment and Repair, Elsevier, 2018: pp. 253–323. https://doi.org/10.1016/B978-0-08-100540-8.00007-8.

[42] International Organization for Standarization, UNE-EN ISO1465:2009, Determination of tensile lap-shear strength of bonded assemblies, 2009.

[43] International Organization for Standarization, UNE-EN ISO 10365:2022, Designation of main failure patterns, 2022.

[44] R. Nazari, M.M. Hatami, A comparative study of the effect of various surface treatments on the fracture behavior of aluminum adhesive joints under mode I loading, Discover Applied Sciences 6 (2024) 1–16. https://doi.org/10.1007/S42452-024-05622-W/FIGURES/13.

[45] T.S.M. Mui, L.L.G. Silva, V. Prysiazhnyi, K.G. Kostov, Surface modification of aluminium alloys by atmospheric pressure plasma treatments for enhancement of their adhesion properties, Surf Coat Technol 312 (2017) 32–36. https://doi.org/10.1016/J.SURFCOAT.2016.08.024.

[46] L. Bónová, A. Zahoranová, D. Kováčik, M. Zahoran, M. Mičušík, M. Černák, Atmospheric pressure plasma treatment of flat aluminum surface, Appl Surf Sci 331 (2015) 79–86. https://doi.org/10.1016/J.APSUSC.2015.01.030.

[47] T.S. Williams, H. Yu, R.F. Hicks, Atmospheric pressure plasma activation as a surface pre-treatment for the adhesive bonding of aluminum 2024, J Adhes Sci Technol 28 (2014) 653–674. https://doi.org/10.1080/01694243.2013.859646.

[48] D. Santiago, D. Guzmán, J. Padilla, P. Verdugo, S. De la Flor, À. Serra, Recyclable and Reprocessable Epoxy Vitrimer Adhesives, ACS Appl Polym Mater 5 (2023) 2006–2015. https://doi.org/10.1021/acsapm.2c02063.

Supporting information for:

Improving the reversible adhesion performance of an epoxy vitrimer adhesive through surface treatment technology

Marc Surós[1,2], Pere Verdugo[1,3], David Santiago[1,2*], Silvia De la Flor[2*]

[1] Eurecat, Technology Center of Catalonia - Chemical Technologies Unit, c/Marcel·lí Domingo 2, 43007 Tarragona, Spain.
[2] Universitat Rovira i Virgili. Department of Mechanical Engineering, Av. Països Catalans 26, 43007 Tarragona, Spain.
[3]Universitat Rovira I Virgili. Department of Analytical and Organic Chemistry, c/Marcel·lí Domingo 1, 43007, Tarragona, Spain.

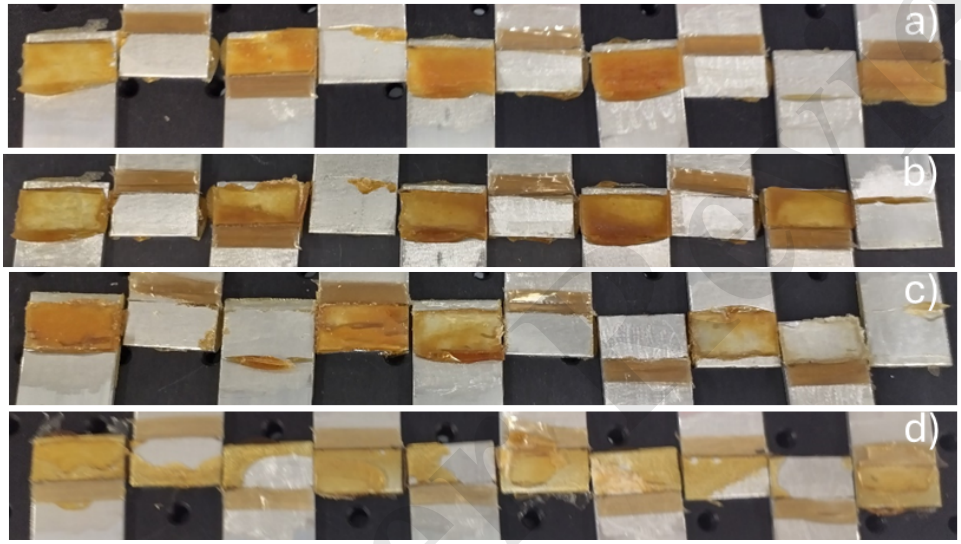

Figure S1. Pictures of the failure surfaces of the different methodologies treated by T0-ref showing an adhesive failure. a) Pristine adhesion, b) re-adhesion after break, c) re-adhesion after debonding and d) adhesion after self-welding.

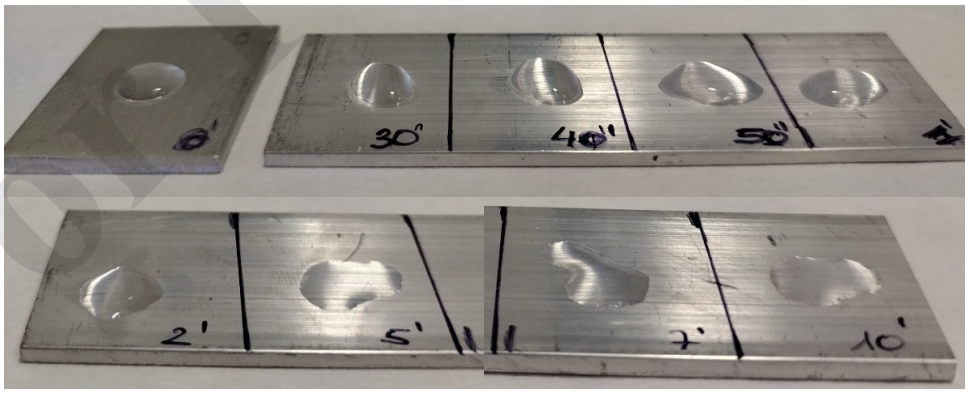

Figure S2. Picture of the aluminum plate used for preliminary plasma tests. A water droplet was placed on each area to visually assess wettability changes. The exposure time was as follows, upper section left to right: 0 s, 30 s, 40 s, 50 s and 1 min. Lower section left to right: 2 min, 5 min, 7 min and 10 min.

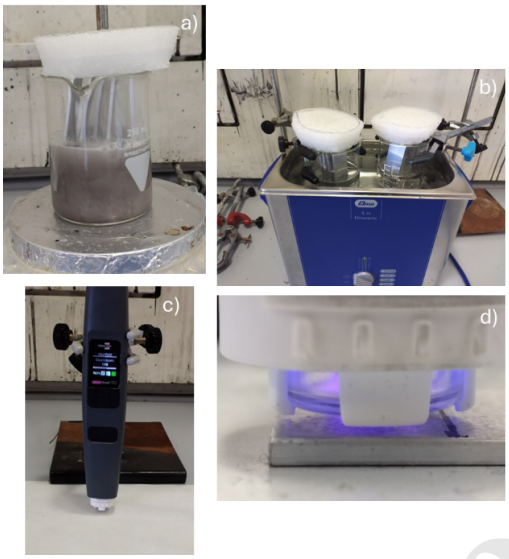

Figure S3. Pictures of the treatment methods used. a) Aluminum plates immersed in an etching solution, b) aluminum plates in an alkaline solution on an ultrasonic bath, c) plasma apparatus on a stand and d) aluminum plate being exposed to plasma.

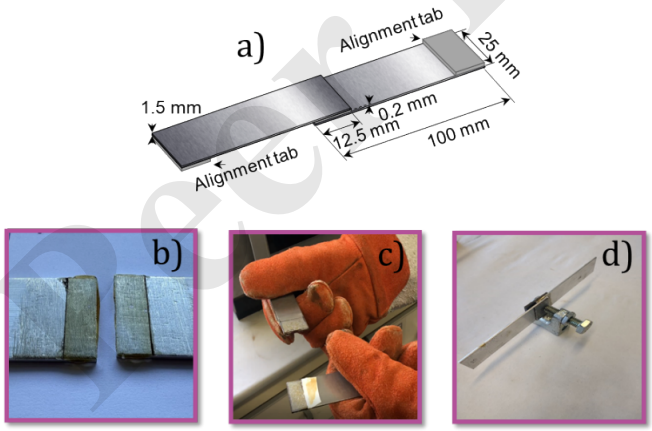

Figure S4. Pictures depicting the adhesion methodologies. a) Scheme of the single lap joint specimens used, b) two aluminum sheets with the adhesive cured on top ready for adhesion after self-welding, c) debonded joint with bare hands and d) re-adhesion set-up.

Table S1. Statistical parameters of the comparisons performed for all treatments in the pristine adhesion methodology.

Rank	Comparison	p value	Critical value	p ≤ 0.05?	p ≤ critical value?	Survives B-H?
1	**S0-S6**	0.001	0.003	Yes	-	Yes
2	**S6-S8**	0.003	0.007	Yes	-	Yes
3	**S0-S7**	0.006	0.010	Yes	-	Yes
4	**S6-S7**	0.008	0.013	Yes	-	Yes
5	**S0-S2**	0.020	0.017	Yes	-	Yes
6	**S0-S1**	0.022	0.020	Yes	-	Yes
7	**S0-S8**	0.023	0.023	Yes	Yes	Yes
8	S0-S4	0.054	0.027	No	No	-
9	S1-S2	0.089	0.030	No	No	-
10	S0-S3	0.121	0.033	No	No	-
11	S3-S4	0.255	0.037	No	No	-
12	S7-S8	0.302	0.040	No	No	-
13	S4-S5	0.434	0.043	No	No	-
14	S0-S5	0.567	0.047	No	No	-
15	S3-S5	0.868	0.050	No	No	-

Tables S1 to S4 show the statistical parameters arising from the statistical analyses performed for each methodology. The Brown-Forsythe test revealed statistically significant differences in variances between the treatment groups. Consequently, Welch's one-way ANOVA was employed to compare the means among each treatment group, giving rise to a p-value for each comparison performed. To control the false discovery rate in multiple comparisons, the Benjamini-Hochberg (B-H) procedure was implemented. In this procedure, the comparisons are ordered according to their p-value in increasing order. Each comparison is assigned a rank from 1 to n. Next, the B-H critical value is obtained from the following equation:

$$Critical\ value = \frac{rank}{n} * Q$$

Where n is the total number of comparisons and Q the chosen discovery rate.

Finally, the p-value and the critical value are compared. The largest p-value that is less than or equal to its critical value is used as a cut-off row. From this value upwards, all comparisons with a p-value lower than or equal to 0.050 survive this correction. In these tables, the cut-off value is designated by a highlighted rank. The values that survive all conditions are painted green, and those that are not found to be statistically significant by any of the two tests are painted red.

Table S2. Statistical parameters of the comparisons performed for all treatments in the re-adhesion after break methodology.

Rank	Comparison	p value	Critical value	p ≤ 0.05?	p ≤ critical value?	Survives B-H?
1	**S4-S5**	0.001	0.003	Yes	-	Yes
2	**S0-S4**	0.002	0.007	Yes	-	Yes
3	**S0-S8**	0.004	0.010	Yes	-	Yes
4	**S0-S5**	0.011	0.013	Yes	-	Yes
5	**S0-S7**	0.012	0.017	Yes	Yes	Yes
6	S0-S6	0.050	0.020	Yes	No	No
7	S3-S5	0.071	0.023	No	No	-
8	S3-S4	0.076	0.027	No	No	-
9	S1-S2	0.135	0.030	No	No	-
10	S6-S8	0.170	0.033	No	No	-
11	S0-S1	0.294	0.037	No	No	-
12	S0-S2	0.384	0.040	No	No	-
13	S6-S7	0.408	0.043	No	No	-
14	S7-S8	0.544	0.047	No	No	-
15	S0-S3	0.790	0.050	No	No	-

Table S3. Statistical parameters of the comparisons performed for all treatments in the re-adhesion after debonding methodology.

Rank	Comparison	p value	Critical value	p ≤ 0.05?	p ≤ critical value?	Survives B-H?
1	S0-S8	0.016	0.006	Yes	No	No
2	S0-S2	0.022	0.013	Yes	No	No
3	S0-S6	0.051	0.019	No	No	-
4	S0-S7	0.062	0.025	No	No	-
5	S6-S8	0.138	0.031	No	No	-
6	S7-S8	0.156	0.038	No	No	-
7	S6-S7	0.854	0.044	No	No	-
8	S0-S4	0.886	0.050	No	No	-

Table S4. Statistical parameters of the comparisons performed for all treatments in the adhesion after self-welding methodology.

Rank	Comparison	p value	Critical value	p ≤ 0.05?	p ≤ critical value?	Survives B-H?
1	**S0-S7**	0.001	0.006	Yes	-	Yes
2	**S6-S7**	0.001	0.013	Yes	-	Yes
3	**S0-S4**	0.003	0.019	Yes	-	Yes
4	**S0-S2**	0.007	0.025	Yes	-	Yes
5	**S0-S8**	0.011	0.031	Yes	-	Yes
6	**S6-S8**	0.012	0.038	Yes	Yes	Yes
7	S7-S8	0.166	0.044	No	No	-
8	S0-S6	0.857	0.050	No	No	-

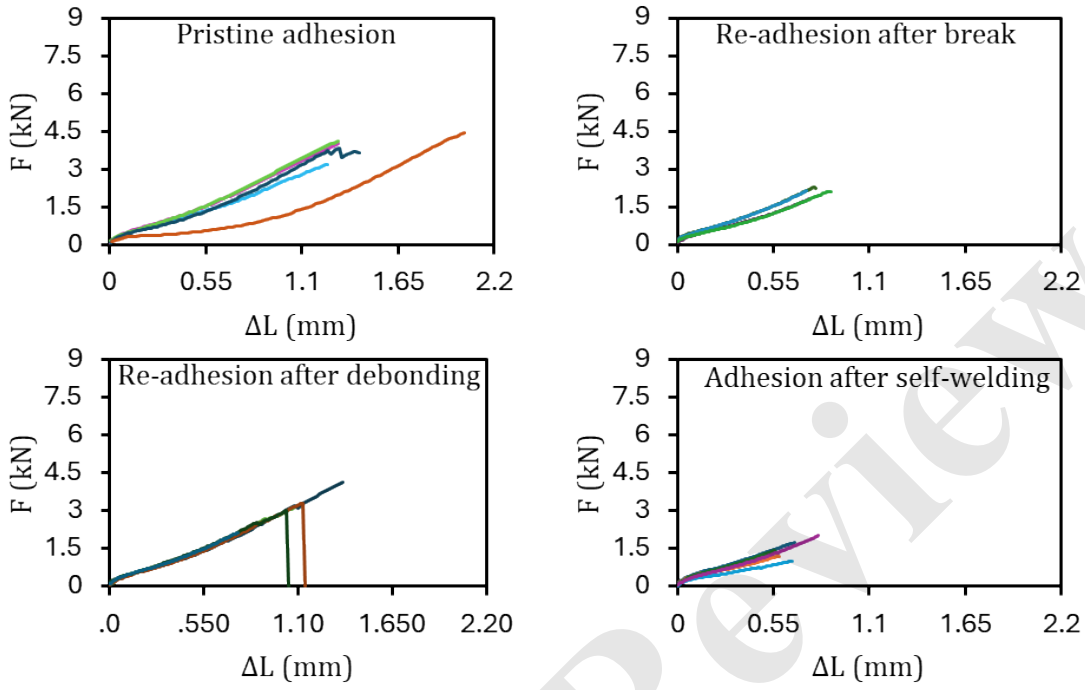

Figure S5. Force-displacement curves of the lap-shear tests of all adhesion methodologies for treatment T0-ref.

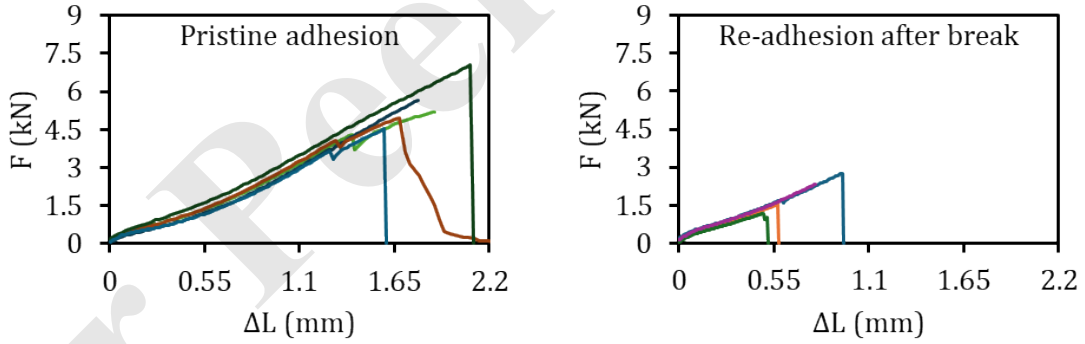

Figure S6. Force-displacement curves of the lap-shear tests of all adhesion methodologies for treatment T1-deg.

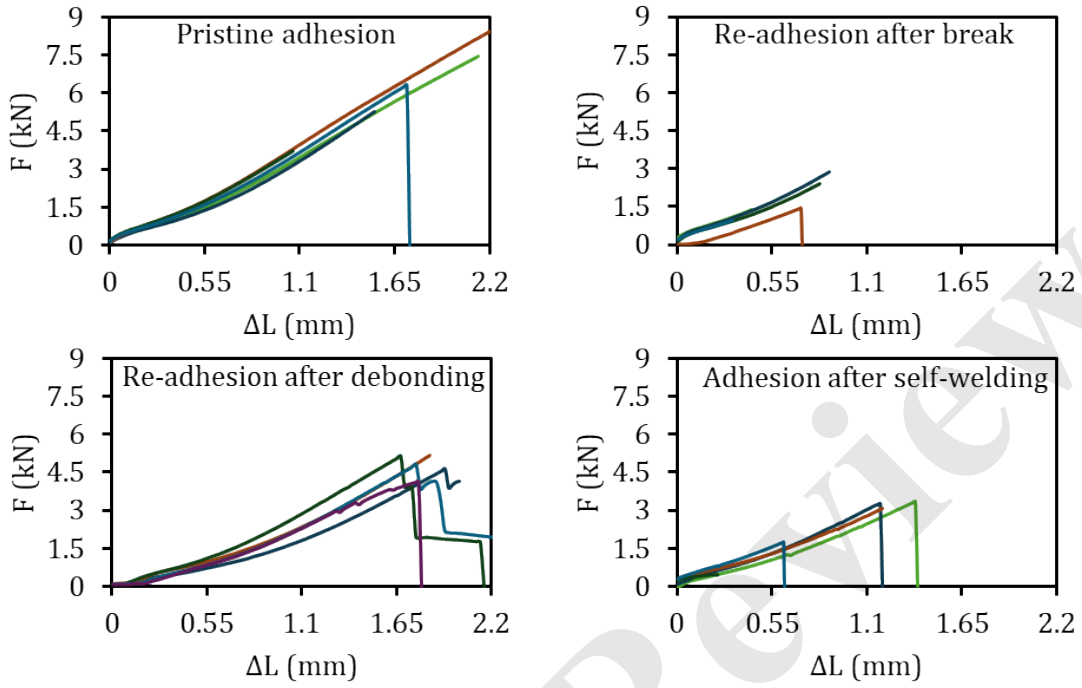

Figure S7. Force-displacement curves of the lap-shear tests of all adhesion methodologies for treatment T2-deg-abr.

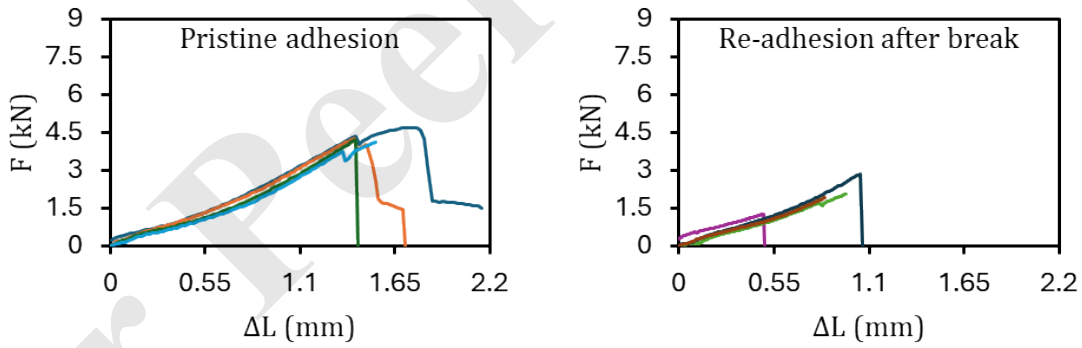

Figure S8. Force-displacement curves of the lap-shear tests of all adhesion methodologies for treatment T3-pla-5.

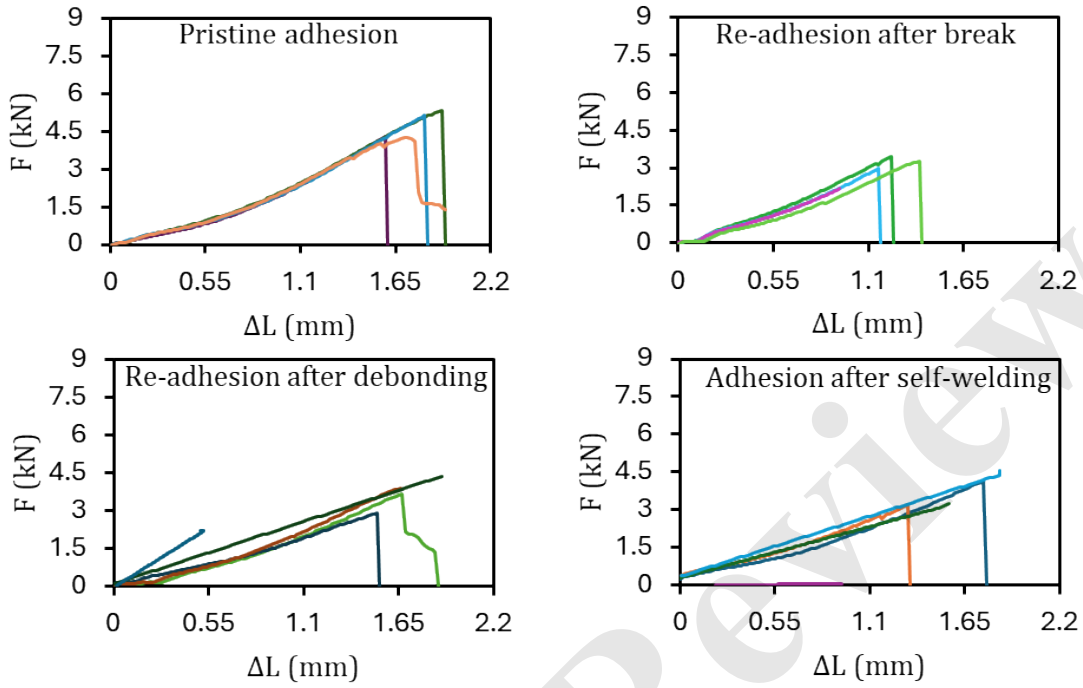

Figure S9. Force-displacement curves of the lap-shear tests of all adhesion methodologies for treatment T4-pla-5-abr.

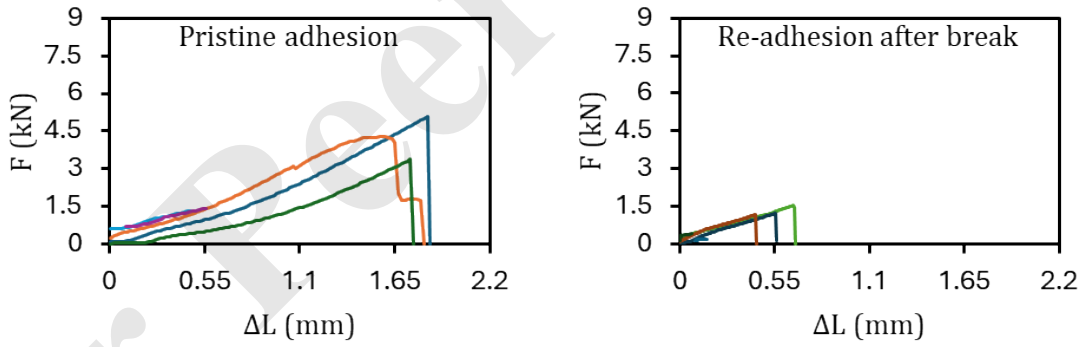

Figure S10. Force-displacement curves of the lap-shear tests of all adhesion methodologies for treatment T5-pla-10-abr.

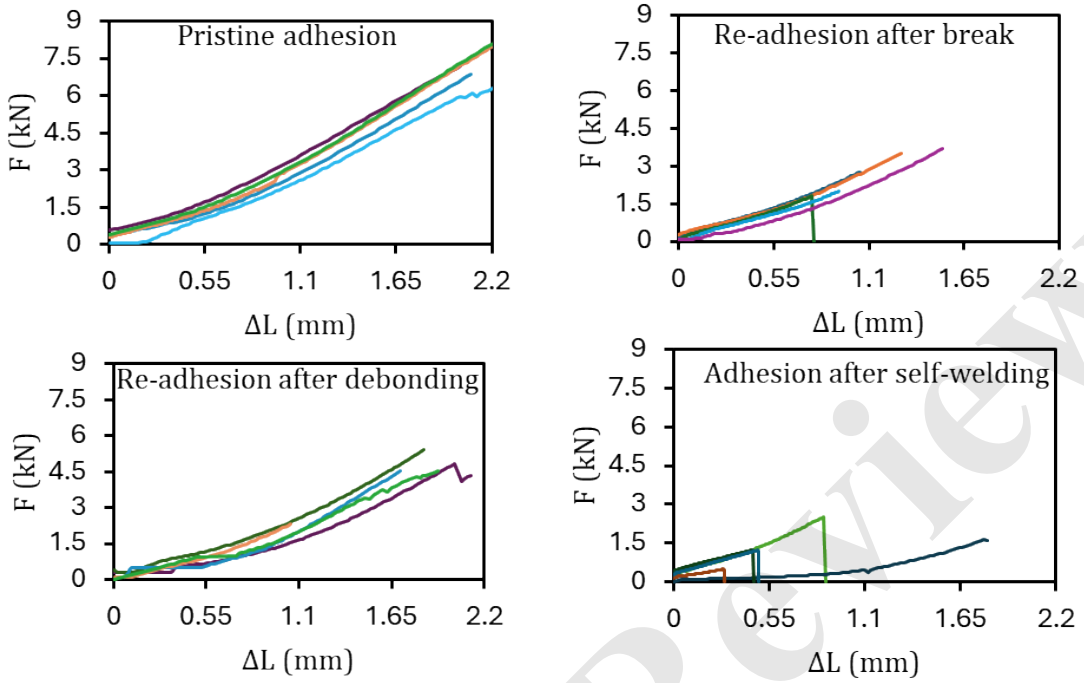

Figure S11. Force-displacement curves of the lap-shear tests of all adhesion methodologies for treatment T6-chem-NO3.

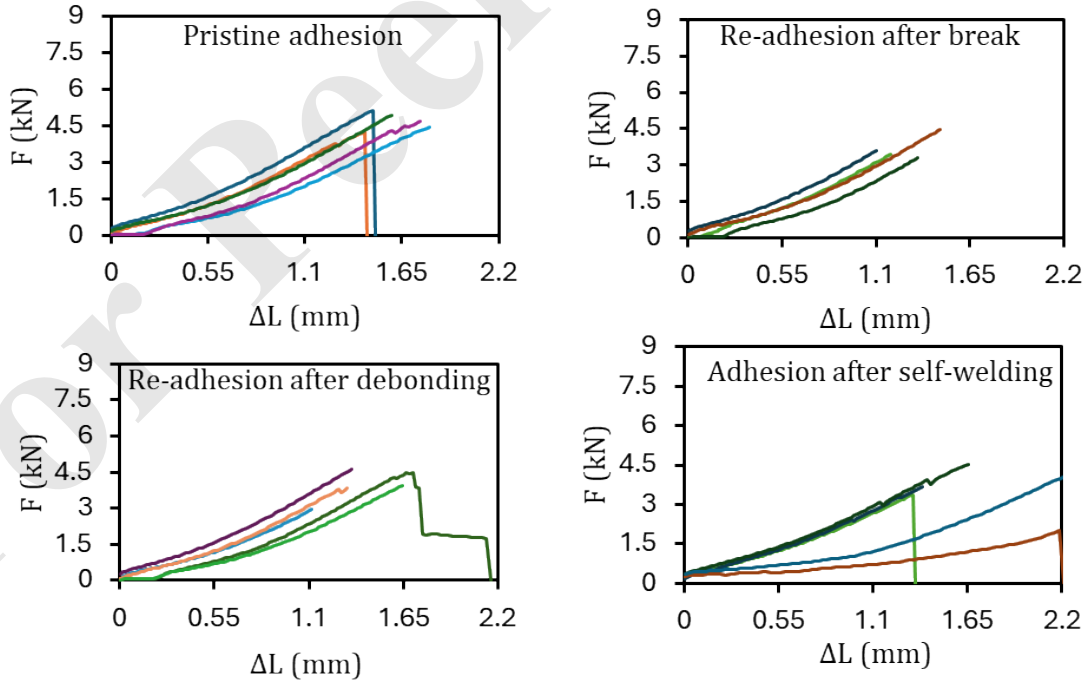

Figure S12. Force-displacement curves of the lap-shear tests of all adhesion methodologies for treatment T7-chem-alkUS.

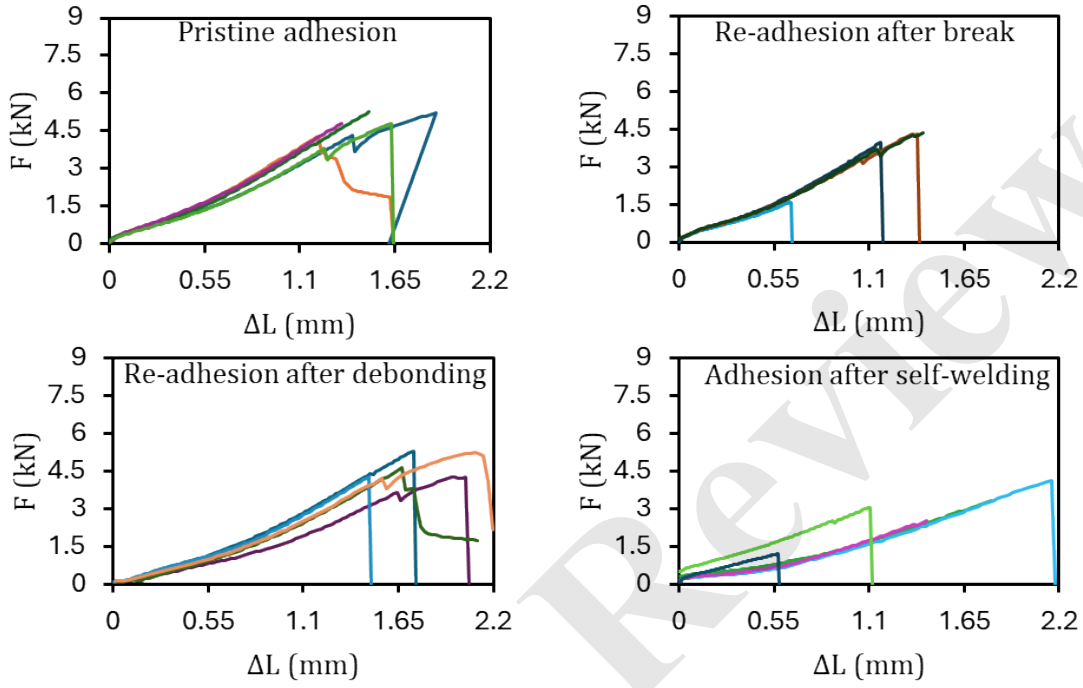

Figure S13. Force-displacement curves of the lap-shear tests of all adhesion methodologies for treatment T8-chem-P2.

Table S5. Microanalysis of samples T0-ref and T2-deg-abr comparing their elemental composition.

Treatment	% Element						
	Al	O	C	Si	Mg	Na	Cl
T0-ref	86.2	10.1	10.1	0.0	0.2	0.1	0.1
T2-deg-abr	92.0	3.2	4.4	0.3	0.2	0.0	0.0

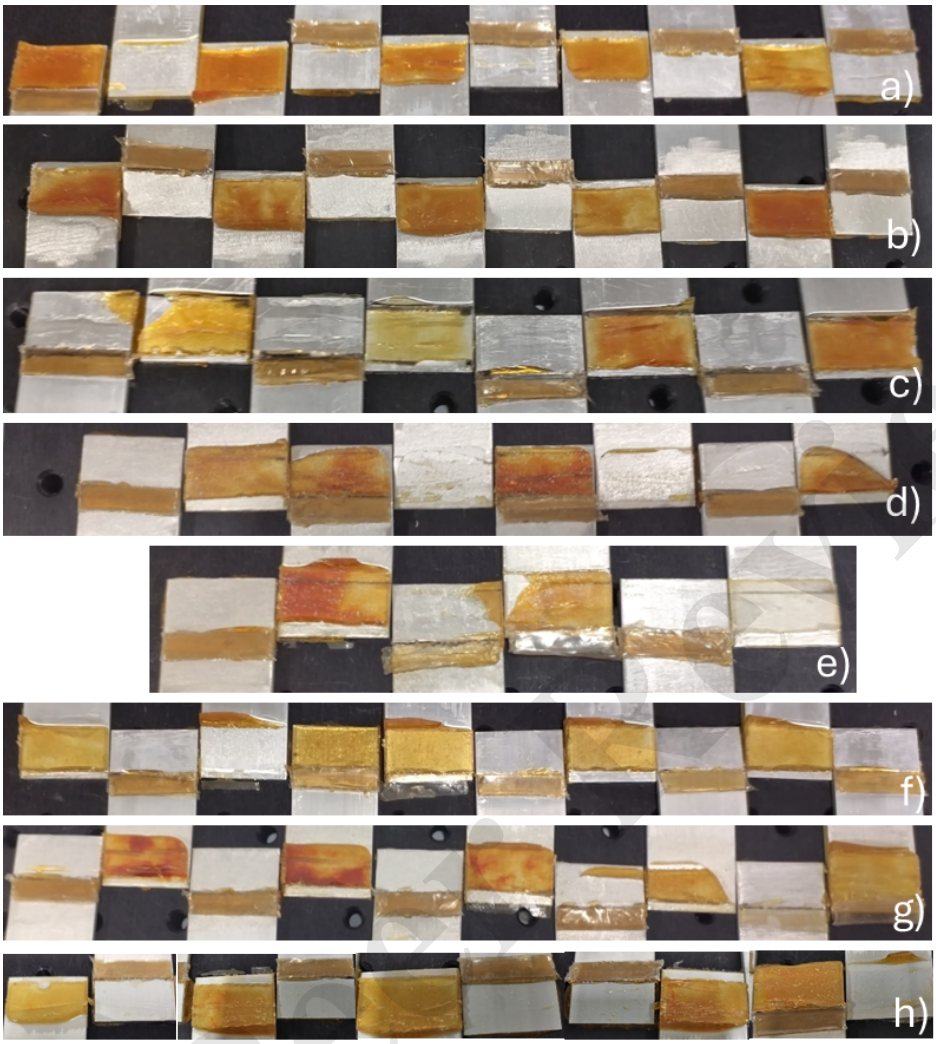

Figure S14. Failure surfaces of pristine adhesions samples for all treatments showing an adhesive failure. a) T1-deg, b) T2-deg-abr, c) T3-pla-5, d) T4-pla-5-abr, e) T5-pla-10-abr, f) T6-chem-NO3, g) T7-chem-alkUS and h) T8-chem-P2.

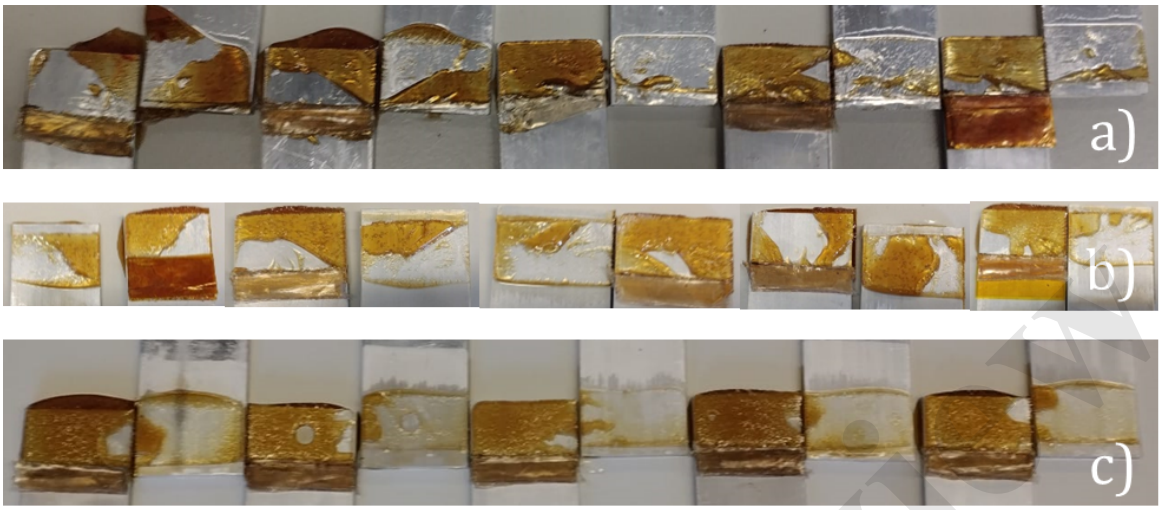

Figure S15. Surfaces of the debonding samples of the chemical treatments after being dismantled by hand, showing a choesive failure. a) T6-chem-NO3, b) T7-chem-alkUS and c) T8-chem-P2.

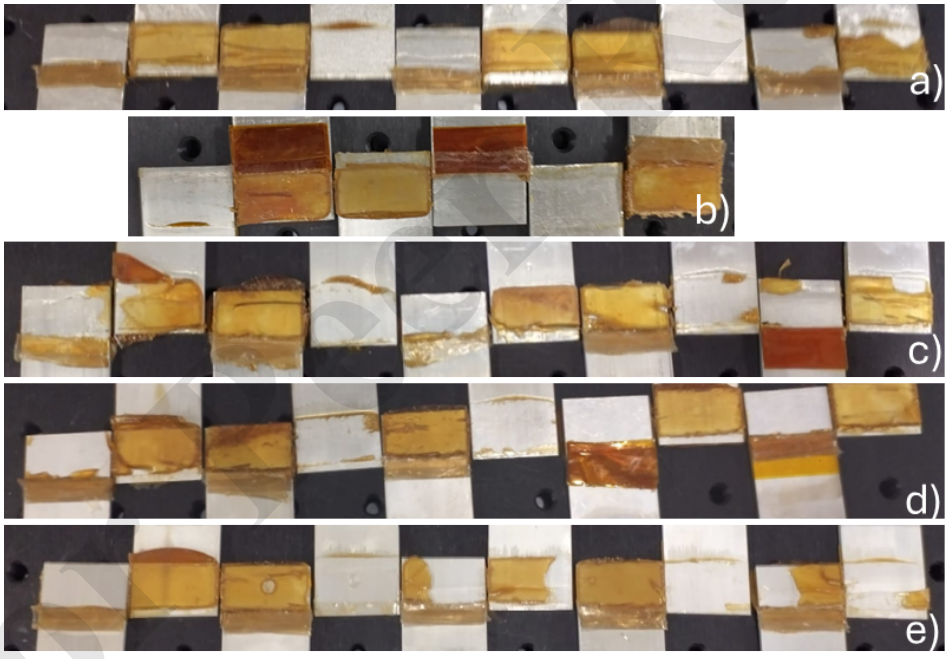

Figure S16. Failure surfaces of the adhesion after debonding samples after being tested. a) T2-deg-abr, b) T4-pla-5-abr, c) T6-chem-No3, d) T7-chem-alkUS and e) T8-chem-P2.

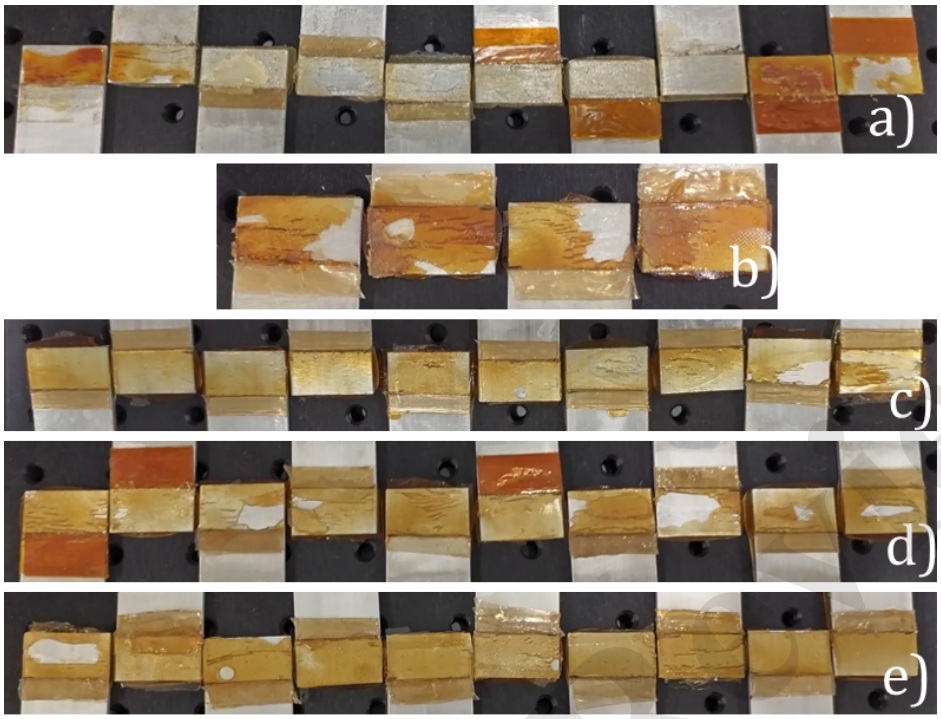

Figure S17. Failure surfaces of the adhesion after self-welding samples for all treatments showing a mostly cohesive failure. a) T2-deg-abr, b) T4-pla-5-abr, c) T6-chem-No3, d) T7-chem-alkUS and e) T8-chem-P2.

Response to reviewers and mention of changes

Dear reviewers,

Thank you once again for taking the time to go through and review our work. We present in this document the responses to all reviewers' comments, including rebuttals as well as the changes made to the manuscript and the supporting information. Furthermore, the changes are highlighted in the manuscript with red font color. We appreciate all comments made by the reviewers as they have let us improve upon our original work and have opened opportunities for fruitful discussion.

Reviewer: 1

Comments to the Author

The authors have accepted and incorporated all of my comments into the paper. Therefore, I recommend the paper for publication.

Reviewer: 2

Comments to the Author

Thank you for your clarification and additions, I believe this manuscript has been improved.

It is undoubtable that the thickness of the bond line influences the strength as evidenced by your previous work. I believe the confusion lay in the discussion on thickness for this study when the thickness of this study was kept constant for all samples. I now understand the comparison of why only the pristine sample had adhesive failure while welding while the other samples had cohesive failure was due to the newly reinforced adhesion forces.

However, why is this not the case for re-adhesion after bonding, when these samples also had the same thickness? I notice you discuss the type of failure after the manual debonding of your samples, but not the failure when testing after the re-adhesion after debonding, and only show the failure of the T0-ref sample in figure S1. Could you expand on these results?

Response

We thank the reviewer for acknowledging our improvements in the original manuscript and their insightful follow-up comments.

Please find below our response:

We understand how the discussion of thickness in this study could be confusing at first, as it was kept constant here. We are glad the revised version helped clarify why this aspect was mentioned.

It is true that we had not previously included pictures of the failure of the debonding samples after testing the re-adhesion. This has been rectified by including them in new Figure S16 of the Supporting information. As can be seen in this figure, the failure is fundamentally adhesive, except for T8-chem-P2 (Figure S17 e)) where some cohesive behavior can be seen. This mostly

adhesive behavior is the same as in the case of the debonding samples of the reference treatment. This is in accordance with the statistical conclusion that the debonding methodology is not greatly affected by surface treatment, but we understand that this can be counterintuitive to the previous reasoning, as they have the same thickness. The key distinction lies in the nature of interface formation.

In the case of self-welding specimens, the adhesion is much more controlled, the forming of the joint happens between two surfaces of adhesive that have been carefully manufactured, and so the only conditioning point is the relaxation properties of the vitrimer (which are kept constant as the same adhesive is always used). In this case, improving adhesion forces yields better adhesion results in a straightforward manner, as discussed previously.

In the case of re-adhesion after debonding, the critical factor is the dismantling of the joint, and particularly, the amount and condition of adhesive that remains on the surfaces after manual separation. This process is inherently less controlled and reproducible, and, presumably, is independent of the surface treatment as shown by the small statistical change in results.

Debonding mechanics in adhesive vitrimers is a vastly unexplored subject, and so for now, this is the best answer we can offer in our first exploratory study. However, we agree that it might be somewhat limited and are excited to research it further in future works.